

# Unusually Large Hysteresis of Temperature-Responsive Poly(*N*-ethyl-2-propionamidoacrylamide) Studied by Microcalorimetry and FT-IR

Mohamed R. Berber,<sup>†</sup> Hironori Mori,<sup>†</sup> Inas H. Hafez,<sup>†</sup> Keiji Minagawa,<sup>†</sup> Masami Tanaka,<sup>‡</sup> Takuro Niidome,<sup>§,||</sup> Yoshiki Katayama,<sup>§,||</sup> Atsushi Maruyama,<sup>⊥</sup> Tomohiro Hirano,<sup>†</sup> Yasushi Maeda,<sup>\*,#</sup> and Takeshi Mori<sup>\*,§,||</sup>

*Division of Life System, Institute of Technology and Science, The University of Tokushima, 2-1 minamijosanjima, Tokushima 770-8506, Japan, Faculty of Pharmaceutical Science, Tokushima Bunri University, Yamashiro, Tokushima 770-8514, Japan, Department of Applied Chemistry, Kyushu University, 744 Moto-oka Nishi-ku, Fukuoka 819-0395, Japan, Center for Future Chemistry, Kyushu University, 744 Moto-oka Nishi-ku, Fukuoka 819-0395, Japan, Institute for Material Chemistry and Engineering, Kyushu University, 744 Moto-oka, Nishi-ku, Fukuoka 819-0395, Japan, and Department of Applied Chemistry and Biotechnology, Fukui University, 3-9-1 Bunkyo, Fukui 910-8507, Japan*

Received: March 25, 2010; Revised Manuscript Received: May 07, 2010

We reported here the full characterization of the hysteresis of the phase transition behavior of an aqueous solution of poly(*N*-ethyl-2-propionamidoacrylamide) (PNEPA), which has a unique  $\alpha,\alpha$ -disubstituted structure, by using microcalorimetry and FT-IR. Phase transition temperatures near the thermodynamic equilibrium were determined by extrapolating the scanning rate of the microcalorimetry to zero. The calculated hysteresis from the phase transition temperature was unusually very large ( $\sim 8$  °C). FT-IR analysis indicated that the large hysteresis of PNEPA resulted from a coupling of intra-/intermonomeric unit hydrogen bonds, which is known to occur in a  $\beta$ -sheet of proteins but has never been reported in temperature-responsive polymers. The effects of the molecular weight and polymer concentration on the hysteresis were studied by using fractionated PNEPAs and it was found that a low molecular weight and a low concentration enhanced the hysteresis.

## Introduction

Aqueous solutions of temperature-responsive polymers show soluble-to-insoluble transitions at their phase transition temperatures.<sup>1</sup> This transition is known to occur rapidly and reversibly in response to a temperature change.<sup>1</sup> These features of the transition are important in polymer applications such as drug delivery systems<sup>2–4</sup> and tissue engineering.<sup>5</sup> However, when the phase transition behaviors in heating and cooling processes are compared, a small retardation in the cooling process versus the heating process is usually observed.<sup>6,7</sup> This retardation is called hysteresis. The hysteresis is mainly due to the cooling process, which includes a kinetically slow dissolution process of each polymer chain from aggregates.<sup>7</sup> Due to the slow kinetics, the hysteresis differs depending on the measurement conditions and techniques employed. Consequently, the hysteresis of temperature-responsive polymers has only been discussed qualitatively.

Zhang et al. recently proposed a method to determine the hysteresis near the thermodynamic equilibrium (quasi-equilibrium).<sup>7,8</sup> They employed dilute concentration (1.0 mg/mL) to suppress the aggregation of polymers, and extrapolated the phase transition temperature determined by high-sensitivity differential scanning calorimetry (DSC) to the zero scanning rate.<sup>7,8</sup> The

determined hysteresis was smaller when compared with reported values which were obtained under nonequilibrium conditions.<sup>7,8</sup> In particular, the hysteresis of a dilute solution of poly(*N*-isopropylacrylamide) (PNIPAM) was determined to be almost zero by their method,<sup>7</sup> showing that quasi-equilibrium conditions can be reached by their method.

Recently, we have reported a unique series of temperature-responsive polymers,  $\alpha,\alpha$ -disubstituted vinyl polymers, which possess two amphiphilic substituents such as an alkylester and an alkylamide at the  $\alpha$ -position of each monomeric unit.<sup>9–11</sup> Because of the two substituents, much diversity of temperature-responsive polymers can be designed when compared with  $\alpha$ -monosubstituted vinyl polymers.<sup>10,11</sup> We previously found that some polymers in this series showed very large hystereses.<sup>12</sup> We speculated that the origin of the hysteresis is due to the high density of the amphiphilic substituents along a main chain, which will enhance the intra-/interchain interactions in the aggregate, and subsequently the dissolution of the polymer chain from the aggregate will be retarded in the cooling process.<sup>12</sup> However, a molecular mechanism to explain the hysteresis and the effects of the molecular parameters on the hysteresis remain poorly understood.

Here we reported a full characterization of an  $\alpha,\alpha$ -disubstituted polymer with a large hysteresis, poly(*N*-ethyl-2-propionamidoacrylamide) (PNEPA). The quasi-equilibrium hysteresis of PNEPA was determined by following the method of Zhang. The effects of important molecular parameters that influence the hysteresis, such as the molecular weight and concentration, were examined. Finally, a molecular mechanism of the hysteresis studied by FT-IR analysis is proposed.

\* To whom correspondence should be addressed.

<sup>†</sup> Division of Life System, Institute of Technology and Science, The University of Tokushima.

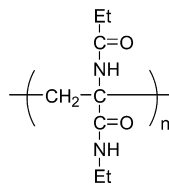
<sup>‡</sup> Faculty of Pharmaceutical Science, Tokushima Bunri University.

<sup>§</sup> Department of Applied Chemistry, Kyushu University.

<sup>||</sup> Center for Future Chemistry, Kyushu University.

<sup>⊥</sup> Institute for Material Chemistry and Engineering, Kyushu University.

<sup>#</sup> Department of Applied Chemistry and Biotechnology, Fukui University.



## Experimental Section

**Materials.** NEPA monomer was synthesized according to our previous report.<sup>12</sup> 2,2'-Azobis(4-methoxy-2,4-dimethylvaleronitrile) (95.0%, Wako) and organic solvents were used as received.

**Polymerization and Fractionation.** NEPA monomer (0.01 mol) and 2,2'-azobis(4-methoxy-2,4-dimethylvaleronitrile) (0.01 mmol) were added to a 100 mL round-bottomed flask, and the resulting mixture was dissolved in 10 mL of chloroform that had been degassed with N<sub>2</sub> prior to use. Polymerization was conducted at 30 °C for 10 h. The polymer was purified by reprecipitation with diethyl ether (yield 80%). Fractionation was performed carefully in a petroleum ether/diethyl ether mixture with a phase-separation technique at room temperature. Three fractions were obtained and denoted as F1, F2, and F3, respectively.  $M_w$  and  $M_w/M_n$  of each fraction are summarized in Table 1.

**Size Exclusion Chromatography.** Molecular weights and molecular weight distributions of the obtained fractions were determined by size exclusion chromatography (SEC) (HLC 8220 instrument, Tosoh Co.) equipped with TSK gels (Super HM-M and Super HM-H, Tosoh Co.) with dimethylformamide (including 10 mM LiBr) as an eluent at 40 °C ([polymer] = 1.0 mg/mL, flow rate = 0.35 mL/min). The SEC chromatogram was calibrated with standard polystyrene samples.

**Determination of Phase Transition Temperature.** Stock solutions of each fraction were prepared with deionized water. Measurement solutions at various concentrations were obtained by further dilution of the stock solutions, and the resulting solutions were maintained overnight in a refrigerator to allow complete dissolution. The transmittance curves of the polymer solutions were recorded at 500 nm with a spectrophotometer (U-3210, Hitachi), equipped with a temperature controller (SPR-10, Shimadzu), operating at various scanning rates. The volume of the solutions and the size of the cuvette were 1.5 mL and 0.5 × 1.0 × 3.0 cm, respectively. The cloud and clearing points ( $T_c$ ) were defined as the temperatures corresponding to 10% reduction of transmittance in a heating process and 10% recovery in a cooling process, respectively.

**High-Sensitivity DSC.** Measurements were performed on a VP-DSC MicroCalorimeter (MicroCal Inc.) with a cell volume of 0.5975 mL under elevated pressure (>28 psi). The sample solution and the reference were degassed at 2 °C for 10 min before use. Three scans were normally measured for each experiment. The data obtained were analyzed with the software provided by the manufacturer based on a non-two-state model.

**FT-IR Measurement.** Details of the method for FT-IR measurements have been described in a previous paper.<sup>13</sup> The copolymer was dissolved in D<sub>2</sub>O to a concentration of  $2.0 \times 10^2$  mg/mL. The copolymer solution (10 μL) was placed between two CaF<sub>2</sub> windows at a path length of 10 μm. The IR cell was attached to a metal cell holder and the temperature was controlled with a circulating water bath. The background spectrum of the first measurement cycle was obtained with a sample solution equilibrated at the starting temperature. IR spectra were then collected continuously while changing the temperature at a rate of ca. 1 deg/min. D<sub>2</sub>O was used as the solvent to avoid the overlapping of amide I and O–H bending of H<sub>2</sub>O.

## Results and Discussion

**Hysteresis at Quasi-equilibrium Conditions.** PNEPA was successfully fractionated by reprecipitation with use of a mixed solvent of petroleum ether and diethyl ether. SEC results of the three fractions (F1, F2, and F3) obtained are summarized in Table 1. The molecular weight distributions of these fractions were relatively narrow.

The transition behavior of F1 at dilute condition (1.0 mg/mL) was observed by high-sensitivity DSC and turbidimetry, and the effect of the scanning rate was examined (Figure 1). Parameters determined by these two measurements are compiled in Table 2. The phase transition temperatures determined by DSC ( $T_p$ ) were consistent with those determined by the turbidimetry ( $T_c$ ). Endothermic peaks in the heating process had symmetrical shapes, and maximum half-widths of the peaks ( $\Delta T_{1/2}$ ) and cooperative monomeric unit lengths ( $n$ ) were constant irrespective of the scanning rate. In contrast, exothermic peaks in the cooling process were not symmetrical and the  $\Delta T_{1/2}$  became larger as the scanning rate increased. The dissolution of aggregates of dehydrated polymer chains has been reported to involve two processes: the swelling of the aggregates as a fast process and the dissociation of the individual polymer chains from the aggregates as a slow process.<sup>7,14</sup> When the scanning rate increased, the slow process of the dissociation of the individual polymer chains will be delayed further when compared to the change in temperature change. This delay was presumed to be the reason for the increase of  $\Delta T_{1/2}$  in Figure 1a.

Following the method of Zhang,<sup>7,8</sup> the phase transition temperature, which is near the equilibration value ( $T_{p0}$ ), was determined by extrapolating  $T_p$  to the zero scanning rate (Figure 2).  $T_{p0}$  in the heating and cooling processes were determined to be 27.2 and 19.5 °C, respectively. Consequently, the hysteresis was calculated to be 7.7 °C. This hysteresis is much larger than those of PNIPAM and poly(*N*-isopropylmethacrylamide) determined by the same method at the same concentration (1.0 mg/mL): ~0 and 1.1 °C, respectively.<sup>7,8</sup>

**TABLE 1: Molecular Parameters for Each Fraction<sup>a</sup>**

fraction	$M_w \times 10^{-4}$	$M_n \times 10^{-4}$	$M_w/M_n$	process	$T_c/^\circ\text{C}$	$T_p/^\circ\text{C}$	$\Delta T_p/^\circ\text{C}$	$ \Delta C_p ^b$	$\Delta T_{1/2}/^\circ\text{C}$	$ \Delta H ^c \times 10^{-3}$	$\Delta H_v^d \times 10^{-5}$	$n^e$
F1	18.2	13.1	1.3	heating	27.5	27.4	8.2	1.33	1.38	2.01	4.80	239
				cooling	19.0	19.2		0.64	2.71	1.97		
F2	9.3	7.4	1.2	heating	28.8	29.1	10.1	1.02	1.36	1.54	4.99	324
				cooling	19.1	19.0		0.41	3.03	1.42		
F3	4.7	3.0	1.5	heating	29.5	29.5	11.1	0.96	1.29	1.47	4.50	306
				cooling	19.3	18.4		0.38	3.22	1.22		

<sup>a</sup> Conditions of DSC and turbidimetry measurements were 1.0 mg/mL and 0.1 deg/min. <sup>b</sup> Peak height (kcal/°C/mol-monomer). <sup>c</sup> Calorimetric enthalpy (cal/mol-monomer). <sup>d</sup> van't Hoff enthalpy (cal/mol-monomer) calculated based on a non-two-state model.<sup>26</sup> <sup>e</sup> Cooperative monomeric unit,  $n = \Delta H_v/\Delta H$ .

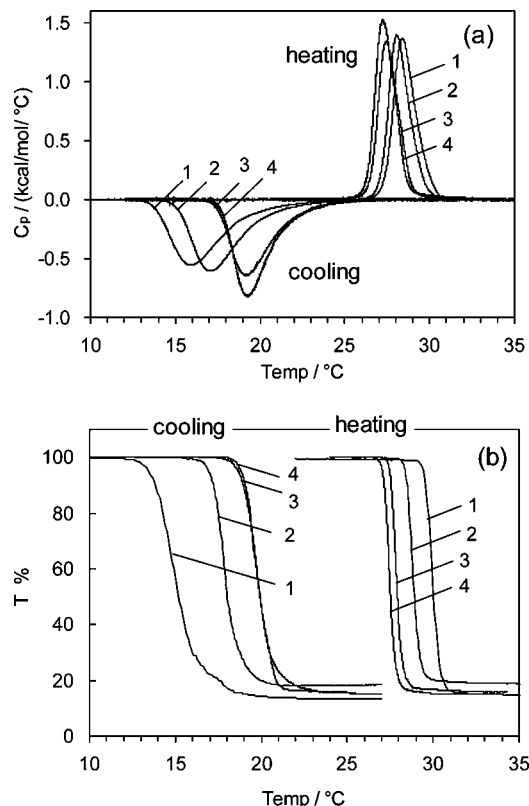


**Figure 1.** Effect of the scanning rate on the phase transition behavior of F1 monitored by high-sensitivity DSC (a) and turbidimetry (b). Scanning rate was 1.0 (1), 0.5 (2), 0.1 (3), and 0.05 deg/min (4), respectively. Polymer concentration was 1.0 mg/mL.

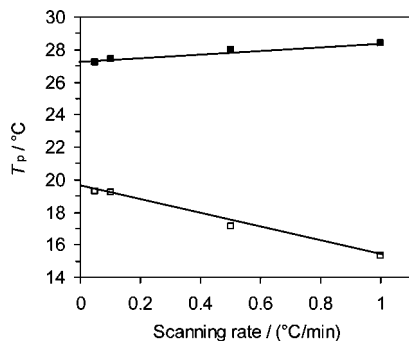


**Figure 2.** Scanning rate dependence of  $T_p$  of F1 in heating (closed square) and cooling processes (open squares). Lines show the extrapolation of  $T_p$  to a zero scanning rate. Polymer concentration was 1.0 mg/mL.

As shown in Table 2,  $\Delta H$  in the heating and cooling processes were essentially consistent with each other even at fast scanning

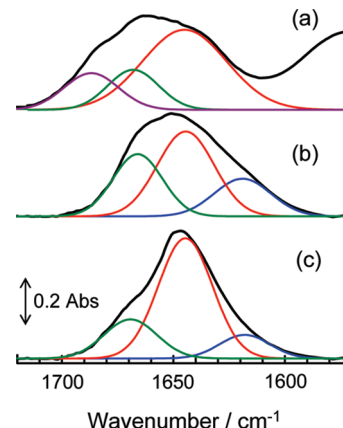


**Figure 3.** IR spectra of a PNEPA cast film (a) and a PNEPA solution below (17 °C, b) and above (50 °C, c) phase transition temperature, and best fitted Gaussian components. In panel a, another peak starting from  $\sim 1610\text{ cm}^{-1}$  resulted from the amide II band of N–H (cast film was prepared without replacing N–H with N–D).

rates. The differences were within 3% irrespective of the scanning rate. This is a clear difference from the results of PNIPAM which showed a 20% difference between  $\Delta H$  in the heating and cooling processes, indicating an incomplete dissolution of the polymer chain in the cooling process.<sup>7</sup> It is interesting to note that PNEPA has rapid dissolution characteristics in spite of its large hysteresis.

**Speculation of Origin of Hysteresis by FT-IR Analysis.** FT-IR spectra can be used to monitor changes in the hydration state of each group during the phase transition. We analyzed the phase transition of PNEPA using FT-IR. D<sub>2</sub>O was used as a solvent instead of H<sub>2</sub>O to avoid the overlapping between the amide I and O–H bending of H<sub>2</sub>O. Figure 3 shows the amide I region of the FT-IR spectra of the PNEPA cast film (a) and PNEPA solution below (b) and above (c) the phase transition temperature. The amide I region mainly results from the C=O stretching vibration. The amide I band of each spectrum was separated into several components by Gaussian fitting, and in total four components were detected. The peak at  $1687\text{ cm}^{-1}$  was observed only in the cast film, and thus the peak should result from the C=O group with no hydrogen bonding (H-bonding). The intensities of the other three peaks in the PNEPA solution changed below and above the phase transition temperature; the peak at  $1645\text{ cm}^{-1}$  increased and the other two peaks ( $1616$  and  $1668\text{ cm}^{-1}$ ) weakened above the phase transition temperature.

To assign each peak, we simulated the IR spectrum of PNEPA. First, 17 kinds of typical structures of the monomeric unit, which forms intra-/intermonomeric unit H-bonding or forms H-bonding with D<sub>2</sub>O, were optimized by a quantum

**TABLE 2: Effect of Scanning Rate on Phase Transition Behavior of F1<sup>a</sup>**

rate/(deg/min)	process	$T_c/^\circ\text{C}$	$T_p/^\circ\text{C}$	$\Delta T_p/^\circ\text{C}$	$ \Delta C_p ^b$	$\Delta T_{1/2}/^\circ\text{C}$	$ \Delta H ^c \times 10^{-3}$	$\Delta H_v^d \times 10^{-5}$	$n^e$
0.05	heating	27.2	27.2	7.9	1.52	1.37	2.27	4.86	214
	cooling	19.0	19.3		0.82	2.56	2.20		
0.1	heating	27.5	27.4	8.2	1.33	1.38	2.01	4.80	239
	cooling	19.0	19.2		0.64	2.71	1.97		
0.5	heating	28.3	28.0	10.9	1.39	1.38	2.17	4.61	212
	cooling	17.1	17.1		0.61	3.12	2.14		
1.0	heating	29.4	28.4	13.1	1.37	1.40	2.23	4.38	196
	cooling	14.3	15.3		0.56	3.40	2.21		

<sup>a</sup> Concentration of DSC and turbidimetry measurements was 1.0 mg/mL. <sup>b</sup> See the same footnote in Table 1. <sup>c</sup> See the same footnote in Table 1. <sup>d</sup> See the same footnote in Table 1. <sup>e</sup> See the same footnote in Table 1.

**TABLE 3: Comparison of Wavenumber of Each Component Obtained by Calculations and Experiments**

	C=O free	C=O...D <sub>2</sub> O	C=O...DN <sub>noncoupling</sub>	C=O...DN <sub>coupling</sub>	C=O...2D <sub>2</sub> O
calcd	1690	1662	1662	1648	1627
obsd	1687	1668	1668	1645	1616

chemical calculation based on a density functional theory (Figure S1, Supporting Information). Then, the IR spectrum for each structure was calculated (Table S1, Supporting Information). In total 35 species of C=O that appeared in the 17 kinds of structures were categorized into five species: C=O with no H-bonding (C=O free), C=O forming H-bonding with one or two D<sub>2</sub>O molecules (C=O...D<sub>2</sub>O and C=O...2D<sub>2</sub>O, respectively), and C=O forming H-bonding with D—N, which coupled with or did not couple with other H-bonding of C=O...D—N (C=O...D—N<sub>coupling</sub> and C=O...D—N<sub>noncoupling</sub>, respectively). The average wavenumbers for the five species are calculated in Table S2 (Supporting Information) and the results are summarized in Table 3. Because the wavenumbers of C=O...D<sub>2</sub>O and C=O...D—N<sub>noncoupling</sub> are superimposable, four peaks will be recognized in the IR spectrum. This result matched the observation, thus the four peaks observed in Figure 3 could be reasonably assigned (Table 3).

During the quantum chemical calculation of 17 kinds of structures, we realized that the monomeric unit has a tendency to form a 7-membered ring as typically shown in Figure 4a. This is the same structure with a  $\gamma$ -turn that is often found in proteins.<sup>15</sup> We also found that a 10-membered ring can be formed through two H-bonds among the remaining C=O and N—H groups of the two monomeric units as shown in Figure 4b. These four H-bonds in the two monomeric units are connected with each other, thereby they couple together and give the sole vibration at 1648 cm<sup>-1</sup> (C=O...D—N<sub>coupling</sub>). The observed peak at 1645 cm<sup>-1</sup>, which increased above the phase transition temperature, will be assigned to this vibration. This kind of coupling of the plural intra/interchain H-bonds is observed in  $\beta$ -sheet structures of proteins,<sup>16</sup> but has never been reported in any temperature-responsive polymers. This unique coupled H-bonded system is most likely the origin of the unusual hysteresis of PNEPA.

Figure 5 shows the temperature dependence of the areas of the three peaks in the amide I region in the heating and cooling processes. As for the heating process, the two peaks resulting from the hydrated species (1616 and 1668 cm<sup>-1</sup>) decreased steeply over a narrow temperature range (27 to 30 °C), whereas the other peak of the intra-/intermonomeric unit H-bonding

(1645 cm<sup>-1</sup>) increased in the same range. This temperature range is almost consistent with those observed by DSC (Figure 1a). It is important to note that even below the phase transition temperature, the peak area of intra-/intermonomeric unit H-bonding is very high compared with that of previously reported polymers, poly(*N*-alkylacrylamide)s<sup>13,17</sup> and poly(*N*-methacrylamide)s.<sup>18</sup> This may indicate the high stability of the intra/interchain H-bonding probably due to the entropic advantage of the 7-membered-ring formation.

As for the cooling process, the hysteresis of the fraction of the peak at 1616 cm<sup>-1</sup> is not clear because of the small change of this fraction, whereas the hystereses of the other two peaks (1645 and 1668 cm<sup>-1</sup>) were clearly observed. Thus, once the intra-/intermonomeric unit H-bonding was formed above the phase transition temperature in the heating process, it remained to be formed until the solution was cooled below the phase transition temperature of the cooling process. It seems that the hysteresis was brought by this intra-/intermonomeric unit H-bonding. The changes of the fractions of the three peaks gradually proceeded in much wider temperature ranges than those of the heating process. This result is consistent with the wider exothermic peaks rather than the endothermic peaks observed by DSC (Figure 1a).

Consequently, we reasoned that the mechanism of the unusual hysteresis of PNEPA is as follows. The unique coupled H-bonding stabilizes the intra/interchain aggregation, thereby resulting in a deep local minimum energy of the aggregate, and the dissolution of polymer chain is consequently extremely slow or a kinetically frozen process. The dispersion of the aggregate is then cooled excessively facilitating hydration over the intra/interchain H-bonding, which finally leads to the dissolution of polymer chain.

**Effect of Molecular Weight.** The molecular weight is well-known to affect the phase transition temperature of the heating process.<sup>19–22</sup> As for the cooling process, however, the effect of the molecular weight remains unsolved. We have studied here the effect of the molecular weight on the phase transition temperature in both the heating and cooling processes and compared the hysteresis of each fraction. Figure 6 shows the DSC trace of the three fractions at a dilute condition (1.0 mg/mL). The *T<sub>p</sub>* value determined from Figure 6 was plotted as a

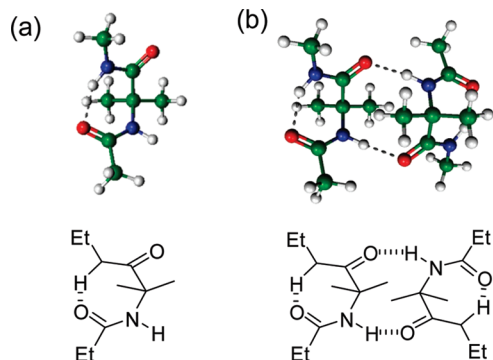


**Figure 4.** Molecular structure of intramonomeric unit (a) and intermonomeric unit (b) hydrogen bonding complexes optimized by quantum chemical calculation. Ethyl groups were replaced with methyl groups for fast calculation because this replacement only showed small differences in the resulting structures.

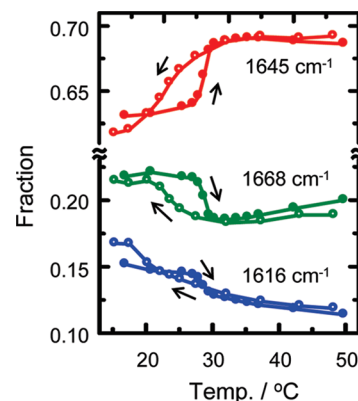


**Figure 5.** Temperature dependence of the area fractions of three peaks of the amide I band in the heating and cooling processes.



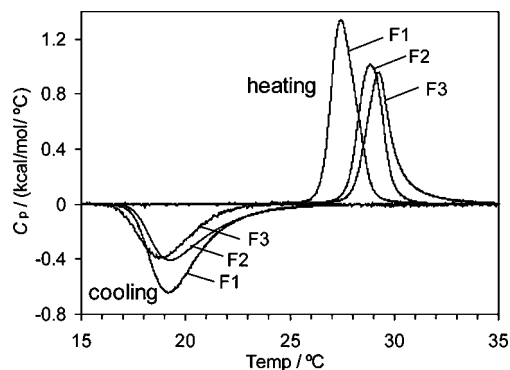


**Figure 6.** Effect of the molecular weight on the phase transition behavior monitored by high-sensitivity DSC. Polymer concentration was 1.0 mg/mL and scanning rate was 0.1 deg/min.

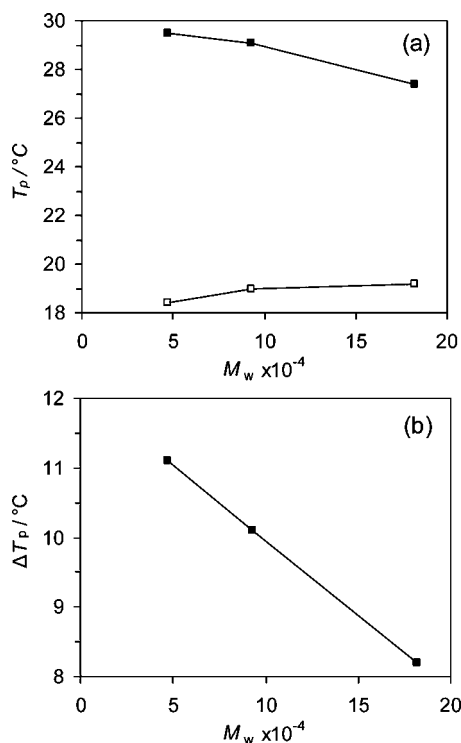


**Figure 7.** Molecular weight dependence of  $T_p$  (a) and hysteresis ( $\Delta T_p$ ) (b). In panel a, closed and open squares indicate  $T_p$  in heating and cooling processes, respectively. Polymer concentration and scanning rate were the same as presented in Figure 3.

function of the molecular weight in Figure 7a.  $T_p$  in the heating process increased with decreasing molecular weight. The same molecular weight dependence has been reported for most of the temperature-responsive polymers.<sup>19,22</sup> This molecular weight dependence will be explained by Flory's equation of state.<sup>23</sup> Because of the dissimilarity of free volume between the polymer and the solvent, the solvent is more expandable than the polymer and therefore the polymer is desolvated at high temperatures. The dissimilarity becomes more obvious for longer polymer chains. Thus, the phase separation of the long chain polymers occurs at lower temperatures.<sup>23</sup>

In contrast,  $T_p$  in the cooling process showed an opposite molecular weight dependence. This is probably because of a stronger interaction in the aggregate of shorter chain. As such, the chains require further cooling for dissociation to occur. A low molecular weight sample has a higher chance for an interchain aggregation in the heating process because it contains

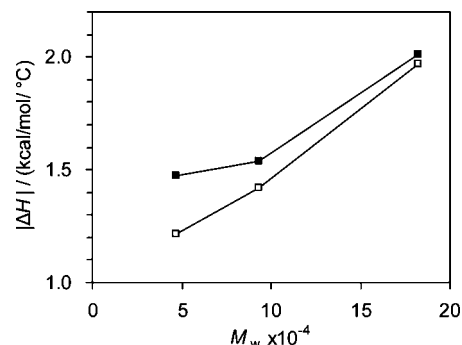


**Figure 8.** Molecular weight dependence of  $\Delta H$  in the heating (closed squares) and cooling processes (open squares), respectively. Polymer concentration and scanning rate were the same as presented in Figure 3.

more chains. The interchain aggregation will be stronger than intrachain contraction because the latter requires bending of the chain, which costs more entropy.<sup>8</sup> Therefore, the lower molecular weight samples showed a lower  $T_p$ . The stronger interchain aggregation in the short chains will be reflected by an increase of  $\Delta T_{1/2}$  in the cooling process with decreasing molecular weight (Table 1).

The observed opposite molecular weight dependence of  $T_p$  in the heating and cooling processes results in the hysteresis ( $\Delta T_p$ ) becoming larger with decreasing molecular weight (Figure 7b). The largest hysteresis observed was  $\sim 11$  °C for F3.

Figure 8 shows the effect of molecular weight on  $\Delta H$ . An absolute value of  $\Delta H$  was found to decrease with decreasing molecular weight. Poly(*N*-isopropylmethacrylamide) showed a similar molecular weight dependence when the  $M_w$  range was the same as the present study ( $M_w < 2 \times 10^5$ ).<sup>8</sup> It was reported that  $\Delta H$  in the heating process is the summation of two processes: the dehydration of the polymer chain (endothermic process) and the formation of the intra/interchain H-bonding (exothermic process).<sup>24</sup> The contribution of the latter process will be enhanced with decreasing molecular weight because of the more effective formation of interchain H-bonding between short chains as explained above. Thus, the overall enthalpy in the heating process will become smaller with decreasing molecular weight. As for the cooling process, smaller  $\Delta H$  in shorter polymer chains will be explained similarly; increasing contribution of the endothermic process (i.e., the dissociation of the intra/interchain H-bonding) in the shorter chains will reduce the overall exotherm.

**Effect of Concentration.** Finally, we compared the effect of the concentration on hysteresis of the long and short polymer chains (F1 and F3). Figure 9 shows the DSC traces at various concentrations (1.0–30 mg/mL). Figure 10a is a plot of  $T_p$  determined from Figure 9 against the concentration. In both fractions,  $T_p$  in the cooling process was almost constant irrespective of the concentration. The constant  $T_p$  in the cooling process was also reported in PNIPAM.<sup>7</sup>

Conversely,  $T_p$  in the heating process showed a clear concentration dependence, especially in the low molecular weight F3;  $T_p$  becomes higher with decreasing concentration. The steeper concentration dependence in the lower molecular weight fraction was also reported in other temperature-responsive polymers.<sup>21</sup> Zhang et al. realized an interesting fact that the concentration dependence of  $T_p$ , which was obtained by extrapolating  $T_p$  to the zero scanning rate, shows an inflection at a chain overlap concentration.<sup>25</sup> Thus, the steeper concentration dependence of F3 than F1 will be reflected in the difference of their overlap concentrations.

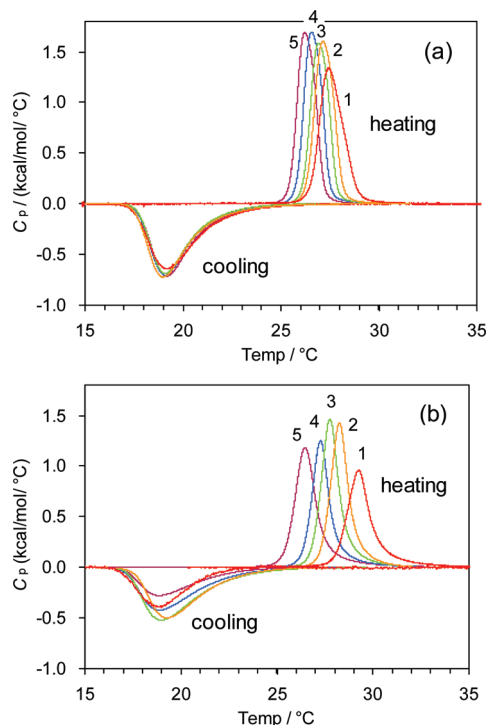


**Figure 9.** Effect of the polymer concentration on DSC traces of F1 (a) and F3 (b). Scanning rate was 0.1 deg/min. Concentrations were 1.0 (1), 5.0 (2), 10 (3), 20 (4), and 30 mg/mL (5), respectively.

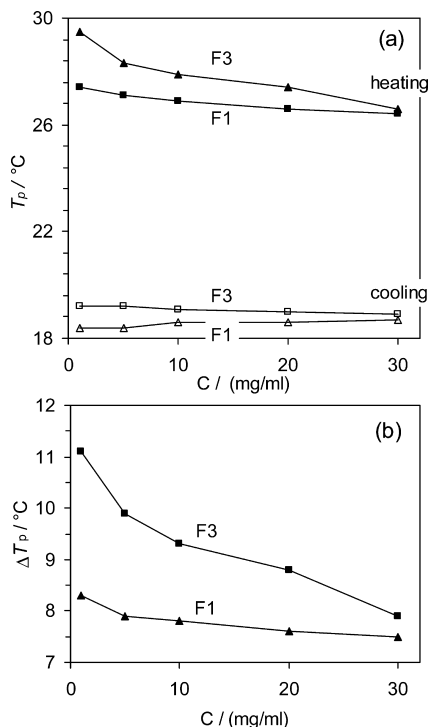


**Figure 10.** Scanning rate dependence of  $T_g$  (a) and hysteresis (b) of each fraction. Scanning rate was 0.1 deg/min.

The difference of  $T_g$  between F1 and F3 became smaller with increasing concentration in both the heating and cooling processes. When the concentration was well above the overlap concentrations, the interchain aggregation was dominant, in which the strength of the interactions will be the same irrespective of the molecular weight.

Figure 10b shows the concentration dependence of the hysteresis of F1 and F3. At the highest concentration (30 mg/

mL), the difference of the hysteresis between F1 and F3 was small because the hysteresis is governed by only interchain aggregation at that concentration. With decreasing concentration, however, low molecular weight F3 showed a steeper increase in the hysteresis than F1, reflecting the difference in their concentration dependence of  $T_g$  in the heating process.

## Conclusions

An aqueous solution of PNEPA showed an unusually large hysteresis even at quasi-equilibrium conditions because of the deep metastability of an aggregate of PNEPA. The molecular origin of the deep metastability was indicated to be a coupling of intra-/intermonomeric unit H-bonds in the aggregate, which has never been reported in other temperature-responsive polymers. Decrease in the molecular weight and the concentration of PNEPA enhanced the hysteresis. PNEPA is a new class of temperature-responsive polymers and its unique solution properties may extend the application field of the temperature-responsive polymers.

**Acknowledgment.** This work was supported in-part by a Grant-in-Aid for Scientific Research (18750152) from the Japanese Ministry of Education, Culture, Sports, Science, and Technology, and by a research grant from NOF Corporation.

**Supporting Information Available:** Results of quantum chemical calculation of structures of monomeric units and their IR spectra. This material is available free of charge via the Internet at <http://pubs.acs.org>.

## References and Notes

- (1) Schild, H. G. *Prog. Polym. Sci.* **1992**, *17*, 163–249.
- (2) Ganta, S.; Devalapally, H.; Shahiwala, A.; Amiji, M. *J. Controlled Release* **2008**, *126*, 187–204.
- (3) Rapoport, N. *Prog. Polym. Sci.* **2007**, *32*, 962–990.
- (4) Wei, H.; Cheng, S.-X.; Zhang, X.-Z.; Zhuo, R.-X. *Prog. Polym. Sci.* **2009**, *34*, 893–910.
- (5) Yamato, M.; Akiyama, Y.; Kobayashi, J.; Yang, J.; Kikuchi, A.; Okano, T. *Prog. Polym. Sci.* **2007**, *32*, 1123–1133.
- (6) Wu, C.; Wang, X. *Phys. Rev. Lett.* **1998**, *80*, 4092–4094.
- (7) Ding, Y.; Ye, D.; Zhang, G. *Macromolecules* **2005**, *38*, 904–908.
- (8) Tang, Y.; Ding, Y.; Zhang, G. *J. Phys. Chem. B* **2008**, *112*, 8447–8451.
- (9) Okamura, H.; Mori, T.; Minagawa, K.; Masuda, S.; Tanaka, M. *Polymer* **2002**, *43*, 3825–3828.
- (10) Mori, T.; Hamada, M.; Kobayashi, T.; Okamura, H.; Minagawa, K.; Masuda, S.; Tanaka, M. *J. Polym. Sci., Part A: Polym. Chem.* **2005**, *43*, 4942–4952.
- (11) Mori, T.; Beppu, S.; Fukushima, S.; Kobayashi, T.; Minagawa, K.; Tanaka, M.; Niidome, T.; Katayama, Y. *Chem. Lett.* **2007**, *36*, 334–335.
- (12) Mori, T.; Beppu, S.; Berber, M. R.; Mori, H.; Makimura, T.; Tsukamoto, A.; Minagawa, K.; Hirano, T.; Tanaka, M.; Niidome, T.; Katayama, Y.; Hirano, T.; Maeda, Y. *Langmuir*. DOI: 10.1021/la100020t. Publication Online: May 13, 2010.
- (13) Maeda, Y.; Nakamura, T.; Ikeda, I. *Macromolecules* **2001**, *34*, 1391–1399.
- (14) Cheng, H.; Shen, L.; Wu, C. *Macromolecules* **2006**, *39*, 2325–2329.
- (15) Vass, E.; Hollósi, M.; Besson, F.; Buchet, R. *Chem. Rev.* **2003**, *103*, 1917–1954.
- (16) Schweitzer-Stenner, R. *J. Phys. Chem. B* **2004**, *108*, 16965–16975.
- (17) Maeda, Y.; Higuchi, T.; Ikeda, I. *Langmuir* **2000**, *16*, 7503–7509.
- (18) Maeda, Y.; Nakamura, T.; Ikeda, I. *Macromolecules* **2001**, *34*, 8246–8251.
- (19) Lessard, D. G.; Ousaleem, M.; Zhu, X. X. *Can. J. Chem.* **2001**, *79*, 1870–1874.
- (20) Xia, Y.; Yin, X.; Burke, N. A. D.; Stover, H. D. H. *Macromolecules* **2005**, *38*, 5937–5948.
- (21) Kunugi, S.; Tada, T.; Tanaka, N.; Yamamoto, K.; Akashi, M. *Polym. J.* **2002**, *34*, 383–388.
- (22) Foryk, S.; Zhang, Y.; Ortiz-Acosta, D.; Cremer, P. S.; Bergbreiter, D. E. *J. Polym. Sci., Part A: Polym. Chem.* **2006**, *44*, 1492–1501.

(23) Tong, Z.; Zeng, F.; Zheng, X.; Sato, T. *Macromolecules* **1999**, *32*, 4488–4490.

(24) Cho, E. C.; Lee, J.; Cho, K. *Macromolecules* **2003**, *36*, 9929–9934.

(25) Ding, Y.; Ye, X.; Zhang, G. *J. Phys. Chem. B* **2008**, *112*, 8496–8498.

(26)  $\Delta H_v$  was obtained by using the calculation program provided by MicroCal Inc. In the program, the equilibrium constant ( $K$ ) at each

temperature ( $T$ ) was first determined by fitting the endothermic or exothermic peak with a non-two-state equilibrium model. Then,  $\Delta H_v$  was obtained from a linear relationship between  $1/T$  and  $\ln K$  based on the van't Hoff equation,  $\ln K = -\Delta H_v/RT + \Delta S/R$  ( $\Delta S$  and  $R$  are entropy and gas constant, respectively).

JP102681Q